

Analytical Noise Treatment for Low-Dose CT Projection Data by Penalized Weighted Least-Square Smoothing in the K-L Domain

Hongbing Lu^{*}, Xiang Li, Ing-Tsung Hsiao, and Zhengrong Liang

Department of Radiology, State University of New York, Stony Brook, NY 11794, USA

ABSTRACT

By analyzing the noise properties of calibrated low-dose Computed Tomography (CT) projection data, it is clearly seen that the data can be regarded as approximately Gaussian distributed with a nonlinear signal-dependent variance. Based on this observation, a penalized weighted least-square (PWLS) smoothing framework is a choice for an optimal solution. It utilizes the prior variance-mean relationship to construct both the weight matrix and the two-dimensional (2D) spatial information as the penalty or regularization operator. Furthermore, a K-L transform is applied along the z (slice) axis to further consider the correlation among different sinograms, resulting in a PWLS smoothing in the K-L domain. As a tool for feature extraction and de-correlation, the K-L transform maximizes the data variance represented by each component and simplifies the task of 3D filtering into 2D spatial process slice by slice. Therefore, by selecting an appropriate number of neighboring slices, the K-L domain PWLS smoothing fully utilizes the prior statistical knowledge and 3D spatial information for an accurate restoration of the noisy low-dose CT projections in an analytical manner. Experimental results demonstrate that the proposed method with appropriate control parameters improves the noise treatment without sacrifice of resolution.

Keywords: Noise reduction, low-dose CT, nonstationary Gaussian noise, Karhunen-Loeve (K-L) transform, penalized weighted least-square smoothing

1. INTRODUCTION

Projection data acquired for image reconstruction of low-dose computed tomography (CT) are degraded by many factors, including Poisson noise, logarithmic transformation of scaled measurements, and pre-reconstruction corrections for system calibration¹. All these factors complicate noise analysis on the projection data and render a very challenging task for noise reduction in order to maintain a high image quality of currently available CT technologies. Considering the low-count nature of this modality with signal dependent noise contamination, conventional approaches for the noise reduction by spatially-invariant, low-pass filters to smooth each projection image separately generate sub-optimal solutions in this situation. Up to now, various forms of filtering techniques have been developed to spatially smooth the projection data and/or the reconstructed CT images¹⁻⁴. One approach models the data noise by Gaussian distribution with variance proportionally depending on the signal or density of the data¹. It utilizes a nonlinear anisotropic diffusion filter to smooth the data noise. Another approach employs an adaptive trimmed mean filter to reduce streak artifacts, which are resulted from excessive X-ray photon noise in low-dose CT projections². Although both of them succeed in some degrees for noise reduction prior to image reconstruction, the assumption of the noise model is not justified in their applications and further development is then limited. Sauer and Liu³ developed a non-stationary filtering method for the anisotropic artifacts in the image reconstruction. Although it utilizes local noise properties to construct a set of non-stationary filters, the method is a post-processing type approach on the images. This type of filtering usually gains noise reduction at the cost of resolution. These previous work on filtering techniques show that, to treat the noise in low-dose CT more accurately, the analysis of the noise properties of pre-corrected CT projection data and the development of a corresponding efficient filtering method are two major problems to be addressed.

In this study, we first investigate the nonlinear noise property of the low-dose CT projection data (after calibration or pre-reconstruction correction) by analyzing a repeatedly acquired experimental data set from a physical phantom at a fixed projection angle. The statistical analysis shows that the noisy calibrated CT projection data can be regarded as

^{*} hblu@clio.rad.sunysb.edu; phone 1 631 444-7921; fax 1 631 444-6450; Dept. of Radiology, State University of New York, Stony Brook, NY 11794-8460, USA.

normally distributed with a nonlinear signal-dependent variance. Based on this observation, the statistical noise properties were incorporated into our technical development of a penalized weighted least-square (PWLS) smoothing framework for an optimal solution. We further integrated the PWLS smoothing into Karhunen-Loeve (K-L) domain for an accurate treatment of the noise in an analytical manner.

2. ANALYSIS OF THE NOISE PROPERTIES

To analyze the noise property of low dose CT data, we first repeatedly acquired projection measurements of a physical phantom at a fixed angle for 900 times by a GE spiral CT scanner. The measurements were calibrated as projection data to satisfy the Radon transform. To make the analysis of the noise property more complete, the phantom was designed to make the acquired measurements cover the practical data range as much as possible. The probability distribution of the calibrated data from channel 600 is shown on the left of Figure 1 with comparison to corresponding Poisson, Gamma, and Gaussian probability distribution functions (PDF). It can be clearly seen that the noise distribution of the projection data has an approximated Gaussian functional, instead of usually assumed Poisson distribution.

The relationship between the variance and the mean of the calibrated data for all the channels is shown on the right of Figure 1. It is clearly seen that the relationship between the data variance and the data mean is nonlinear and may not have an analytical functional formula.

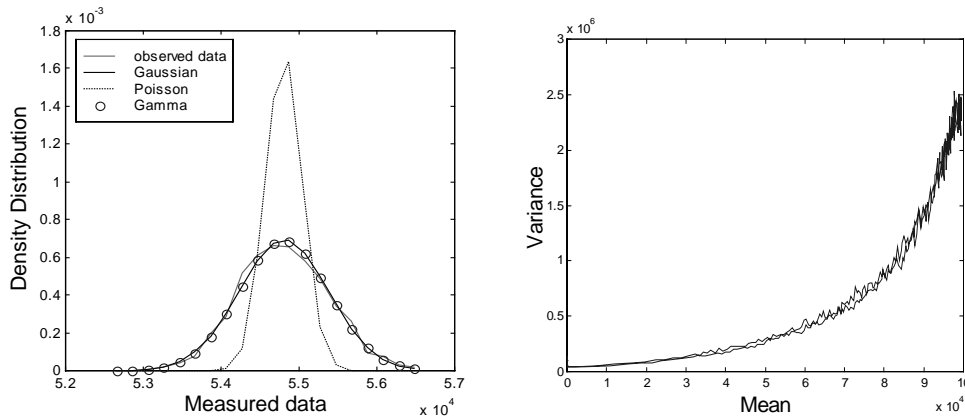


Figure 1: Noise property of acquired low-dose CT projection data. The number of channels per view is 888 and the number of measurements is 900. Left: PDFs of channel 600. Right: Variance-mean curve.

3. K-L DOMAIN PENALIZED WEIGHTED LEAST-SQUARE SMOOTHING

3.1 Penalized Weighted Least-Square Criterion for Smoothing

As we know, statistical estimation approaches have the advantages of modeling the noise nature and providing an optimal solution for the projection means consistent with the objective criterion. Given the Gaussian functional of noise property and the mean-variance relation, we could use a penalized weighted least square criterion, which is optimal for normally distributed data with unequal variances, for a practical solution. Motivated from the experiences with penalized weighted least-squares reconstruction⁵, Fessler described a nonstationary sinogram smoothing method based on an information-weighted smoothing spline⁶. The method estimates a curve fitting to each projection by minimizing a roughness-penalized, weighted least squares (WLS) objective function in which the weights are determined from both the calibration factors and the measurements themselves.

The PWLS criterion used in this study is similar to the spline smoothing method described by Fessler⁶. In general, PWLS smoothing criterion estimates ideal projection by minimizing the following cost functional:

$$\Phi(p) = \frac{1}{2}(y - Hp)^T \Sigma^{-1}(y - Hp) + \beta R(p) \quad (1)$$

in which y is a vector of pre-corrected measurements (i.e., calibrated, pre-reconstruction, to be corrected by this presented method) y_i , p represents the ideal sinogram, Σ is the diagonal variance matrix of y , H is system matrix that describes the blur in sinograms, and T denotes transpose operation. An adjustable parameter β is introduced for the regularizing penalty term $R(p)$ to control the degree of smoothness. Minimizing $\Phi(p)$ means a tradeoff between the

smoothness and a weighted agreement with the measurements, where the smoothing parameter β controls that tradeoff. In this study, we use a quadratic penalty:

$$R(p) = \frac{1}{2}(p - \mu)^T W^{-1}(p - \mu) \quad (2)$$

where $\mu = E[p]$, and the matrix W^{-1} , known as the regularization operator, determines the nature of the smoothing.

3.2 Spatial K-L Transform

As a tool for feature extraction and de-correlation, the K-L transform manipulates a sequence of correlated measurements into an uncorrelated, ordered principal component series, each of which maximizes the data variance, and therefore provides a unique means for noise reduction, feature extraction and de-correlation^{9,10}. Recently, K-L transform has been extensively studied in the field of tomographic reconstruction¹¹⁻¹⁴. For example, Wernick *et al.* attempted to improve the computational speed of spatio-temporal image reconstruction by discarding the higher order components in K-L domain^{11,12}. The digital phantom results were very encouraging, though, the experimental results seemed not so satisfactory when the method was applied to patient data, as shown in their reports.

For 3D spatial filtering, the K-L transform can be applied spatially along the direction of slices or views. Its forward and inverse formula are defined as:

$$\text{K-L transform:} \quad \hat{y} = A_M y \quad (3)$$

$$\text{Inverse K-L transform:} \quad \hat{p} = A_M^T \hat{y} \quad (4)$$

where y is the calibrated projection data. $A_M = A \otimes I_M$. A is the K-L basic vectors which can be obtained as the eigenvectors of the spatial covariance matrix K_t ($K \times K$) calculated from the total K neighboring slices or views, and $K_t A^T = A^T D$. D is a diagonal matrix of eigenvalues d_i . I_M denotes the $M \times M$ identity matrix and \otimes represents the Kronecker product.

In K-L domain, we have

$$\hat{y} = A_M y = A_M H p + A_M n = H p' + \hat{n}, \quad (5)$$

where $\hat{n} = A_M n$, $p' = A_M p$ is K-L transformed ideal data. By K-L transform, the components in K-L domain are independent and remain the same form as in spatial domain. Thus many estimation methods deduced in the spatial domain may be still applicable in the K-L domain. On the other hand, since the information in K-L domain sinograms decreases monotonically from the lower order components to higher order components, the high-order K-L components could be discarded for further noise removal to save the computing time, without losing noticeable information.

3.3 Penalized Weighted Least-Square Smoothing in K-L Domain

The motivation for K-L domain PWLS is based on the following facts. Firstly the ideal projection data between neighboring slices or views are greatly correlated. Treating the sinograms slice-by-slice or view-by-view would ignore the spatial correlation along the direction of slices or views. Secondly, with the de-correlation feature, K-L transform simplifies the complex task of three-dimensional (3D) filtering into 2D spatial process series separately. Finally, since in K-L domain, all components are arranged according to their variance, high-order KL components could be discarded for further noise removal and time saving.

Recently, based on the PWLS principle and K-L transform, Wernick, *et al.* have proposed an optimal pre-reconstruction filtering method and a spatial-temporal reconstruction algorithm for dynamic PET, attempting to take the correlation between the time sequences into account and to improve the computational speed of spatio-temporal image reconstruction by discarding the higher order components in K-L domain^{11,12}. The basic principles used in Wernick's method are similar to ours, except that what our emphases are the spatial correlation existed in projection data and the nonlinear Gaussian distribution property of low-dose CT noise. Therefore the proposed method could be employed more widely in other applications.

The proposed K-L domain PWLS smoothing technique is based on the following assumption: if the regularization operator is chosen to be separable into two components (separability assumption) as

$$W^{-1} = [K_t \otimes W^{2D}]^{-1}, \quad (6)$$

then the PWLS cost functional in Eq.(1) can be greatly simplified into K independent functions in K-L domain:

$$\Phi_l(\tilde{p}_l) = \frac{1}{2}(\tilde{y}_l - H_l \tilde{p}_l)^T \tilde{\Sigma}_l^{-1}(\tilde{y}_l - H_l \tilde{p}_l) + \frac{1}{2} \left(\frac{\beta}{d_l}\right) (\tilde{p}_l - \tilde{\mu}_l)^T [W^{2D}]^{-1} (\tilde{p}_l - \tilde{\mu}_l) \quad l=1, \dots, K. \quad (7)$$

where \tilde{p}_l , \tilde{y}_l , and $\tilde{\mu}_l$ are the l -th K-L components of p , y , and μ , respectively. Notation $\tilde{\Sigma}$ is the diagonal variance matrix of \tilde{y}_l , and d_l is the eigenvalue associated with the l -th K-L vector^{11, 12}.

It's clearly that Eq. (7) is quadratic in \tilde{p}_l . Based on the Gaussian likelihood assumption, we have explicitly the estimation of projection data in K-L domain as:

$$\hat{\tilde{p}}_l = (H_l^T \tilde{\Sigma}_l^{-1} H_l + \left(\frac{\beta}{d_l}\right) [W^{2D}]^{-1})^{-1} H_l^T \tilde{\Sigma}_l^{-1} \tilde{y}_l \quad (8)$$

It is noted that unlike spatial domain PWLS, β/d_l is used as smoothing parameter in K-L domain PWLS. The system matrix H_l describes the blurring in each individual sinogram. In this study, we simply set it equal to identity matrix to ignore the blurring effect in the low-dose CT projections.

By selecting an appropriate number of neighboring slices or views within the CT projection data, the K-L domain PWLS smoothing could fully utilizes the prior statistical knowledge and 3D spatial information for an accurate estimation from the noisy low-dose CT projections.

3.4 Parameters Determination and Procedure Summary

3.4.1 Estimation of Σ^{-1}

We rely the weights Σ on estimates of the variance computed from above variance-mean curve and the measurements themselves. A curving fitting is first applied to match the above variance-mean curve with an appropriate function. For a given pixel (for a simplified case in two dimensions), a 3×3 or 5×5 mean filter is used to get an estimate of the data mean. The estimated data variance is then calculated by inserting the estimated mean into the fitting function. Since this estimate may be unreliable for very small y_l , a small threshold $K > 0$ is then utilized for a sensible weighting.

3.4.2 Neighborhood Selection

It is commonly recognized that the farther away the two slices or views are, the less the correlation is. In our study, we tried to select 3 - 9 neighbors to perform K-L transform along the direction of slices or views. After an appropriate number of neighbor slices or views (K) is selected, the covariance matrix K_l of projection data can be estimated from¹¹

$$K_{l;kl} = \frac{1}{M-1} \sum_{i=1}^M (y_{k,i} - \bar{y}_k)(y_{l,i} - \bar{y}_l) \quad (9)$$

where

$$\bar{y}_k = \frac{1}{M} \sum_{i=1}^M y_{k,i}, \quad k, l = 1, \dots, K \quad (10)$$

3.4.3 Determination of Penalty Term

The penalty or regularization embedded in the cost functional determines the nature of the smoothing. In our study, we chose $[W^{2D}]^{-1}$ to be QTQ , where Q is a block-circulant matrix representing a discrete approximation of the 2D Laplacian operation. For one-dimensional cases, multiplication by $[W^{2D}]^{-1}$ is equivalent to convolve each row of the sinogram with the kernel $[-4 \ 6 \ -4]$. In this situation, Eq. (8) is easily and rapidly computed as a row-by-row operation on the K-L sinograms. If the membrane prior is used as 2D spatial regularization operator (smoothing prior), multiplication by $[W^{2D}]^{-1}$ is equivalent to convolve the sinogram with the kernel $\begin{bmatrix} -\sqrt{2} & -2 & -\sqrt{2} \\ -2 & 8+4\sqrt{2} & -2 \\ -\sqrt{2} & -2 & -\sqrt{2} \end{bmatrix}$.

The smoothing parameter β controls the degree of smoothness in the PWLS criterion. However, for K-L domain PWLS, β/d_l is used as smoothing parameter, where d_l is the eigenvalue of the l -th K-L domain sinogram component. It suggests that K-L components with small eigenvalues would be smoothed intensively or be discarded for fast computation.

3.4.4 Procedure Summary

The implementation procedure of our proposed method for noise treatment of low-dose CT projection data is summarized as follows:

- ◆ Compute the 1D spatial covariance matrix K_f from selected number of neighboring slices or views according to Eq.(9). It would be very fast because the number is small.
- ◆ Calculate K-L transform matrix A from K_f based on $K_f A^T = A^T D$.
- ◆ Apply spatial K-L transformation on selected neighboring projection data.
- ◆ Restore the K-L domain sinograms or projections by the PWLS criterion separately.
- ◆ Apply inverse K-L transformation on the restored data by $A M'^T$, with high-order K-L components discarded.
- ◆ Normalize smoothed projection data.
- ◆ Reconstruct images by conventional filtered backprojection (FBP) method.

4. EXPERIMENTAL RESULTS

Experimental phantom projections acquired by the same GE spiral CT scanner with fan-beam curved detector array were used to evaluate this proposed smoothing method. The phantom is a cylinder with several small details, as shown on the top left of Figure 2. The number of channels per view is 888 with 984 views evenly spanned on a circular orbit of 360° . The detector array is on an arc concentric to the X-ray source with a distance between the X-ray source and the rotation center equal to 541 mm. The distance from the rotation center to the curved detector is 408.075 mm. The detector cell spacing is 1.0239 mm. After system calibration, the calibrated projection data were filtered by different kinds of smoothing methods (including ours) for comparison purpose prior to image reconstruction. The filtered projection data were then reconstructed by the conventional FBP method with the Ramp filter.

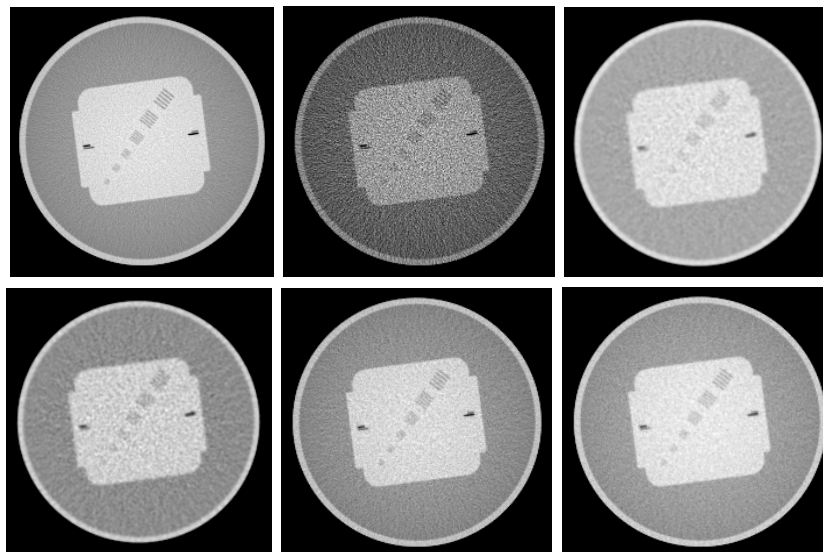


Figure 2: Comparison of FBP reconstructed CT images using different filtering approaches. Top from left to right: noise-free result, noisy data result with Ramp filter, Hanning Filter (cutoff frequency f_c is 0.25). Bottom from left to right: Hanning filter ($f_c = 0.40$), K-L domain PWLS with pc (number of principal components) = 5, $\beta = 5$; K-L domain PWLS with $pc = 3$, $\beta = 20$.

To illustrate the drawbacks of conventional stationary filters and the potential advantages of nonstationary smoothing, the reconstructed slices obtained using different filtering approaches are shown in Figure 2. The “noise-free” data come

from the average of 19 repeatedly acquired datasets, while the “noisy data” come from a single dataset. Compared with images obtained from currently available CT modalities, the noise level appeared in the noisy reconstructed image of low-dose CT looks quite high (top middle of Figure 2). The reconstructed images filtered by the Hanning filters with different cutoff frequencies reveal the tradeoff between image resolution and noise. Insufficient noise suppression was observed for higher cutoff frequencies. For lower cutoff frequencies, image resolution is sacrificed. Unfortunately, whether the cutoff frequency is higher or lower, the small lines and details in the phantom are hardly visible when Hanning filters was applied. For reconstructed images filtered by our K-L domain PWLS, the result obtained by selecting 5 neighboring slices (views) with smoothing parameter $\beta = 5$ are shown in the bottom middle of Figure 2. It outperforms that on the bottom right of Figure 2 obtained by selecting 3 neighboring slices with $\beta = 20$. However, the clearly visible edges and contours appeared in the two images demonstrate that the proposed method outperforms Hanning filters over a range of cutoff frequencies. It shows that the proposed method with appropriate control parameters provides a significant improvement on noise suppression than the low-pass filters, such as Hanning filter, without sacrifice of the spatial resolution.

Application of the proposed K-L domain smoothing scheme to the experimental projection data yields the component images as shown in Figure 3 when five neighboring slices are selected. The superior performance of this scheme in ordering the K-L components by image quality is apparent. Compared with K-L domain component image 1, component images 2 and 3 are almost dominated by noise. Therefore after PWLS smoothing in K-L domain, the high order K-L components could be discarded for further noise removal.

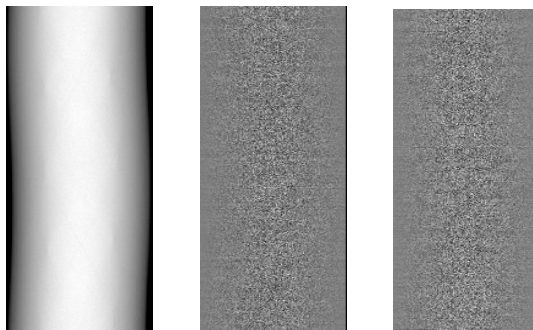


Figure 3: K-L domain component images. From left to right: component image 1, 2, 3, corresponding eigenvalues ($p_c = 5$): $d_1=3.75 \times 10^9$, $d_2=1.19 \times 10^6$, $d_3=1.13 \times 10^6$, respectively.

5. DISCUSSION AND CONCLUSION

In this study, we investigated the non-stationary noise properties of low-dose CT projection data and presented a smoothing framework that takes the statistical natures into account. The noise properties of low-dose CT modality are analyzed by repeatedly acquired experimental phantom datasets. As claimed by many investigators before, it is signal-dependent. However, the noise distribution of the projection data has an approximated Gaussian functional, instead of usually assumed Poisson distribution. The relationship between the data variance and the data mean is nonlinear and may not have an analytical formula.

Considering the Gaussian functional and the mean-variance relation of the low-dose CT projection data shown in Figure 1, we have proposed an K-L domain PWLS smoothing scheme for an alternative optimal solution. It accounts for not only the prior knowledge of the noise properties, especially the relative variance of each detector measurement, but also the 3D spatial information. Thus it significantly improves the tradeoff between bias and variance. The described method is an attempt to capture the benefits of statistical modeling in a non-iterative manner. Since it is an analytical method with computational efficiency, more accurate treatment of non-stationary noise can be achieved by the proposed technology without intensive computational load.

Since no attempt is made to deconvolve a spatially-variant system response, we expect that the described method will be appropriate for systems that have nearly spatially-invariant detector response and nonstationary variance, which has

been verified in low-dose CT case. Our analytical noise treatment provides a theory-based efficient means for low-dose CT modality. This may change the whole spectrum of CT applications in clinic.

ACKNOWLEDGEMENTS

This work was supported in part by the NIH National Heart, Lung and Blood Institute under Grant No. HL54166 and National Cancer Institute under Grant No. CA82402. The authors greatly acknowledge Dr. J. Hsieh, who is with Applied Science Laboratory of GE Medical Systems, for providing the phantom experimental projection data for the noise analysis and evaluation of proposed method.

REFERENCES

1. K. Demirkaya, "Reduction of noise and image artifacts in computed tomography by nonlinear filtration of the projection images", *SPIE Med. Imaging*, **4322**, pp. 917-923, 2001.
2. J. Hsieh, "Adaptive streak artifacts reduction in computed tomography resulting from excessive x-ray photon noise", *Med. Physics*, **25**, pp. 2139-47, 1998.
3. K. Sauer and B. Liu, "Non-stationary filtering of transmission tomograms in high photon counting noise", *IEEE Trans. Med. Imaging*, **10**, pp. 445-452, 1991.
4. C.L. Chan, A.K. Katsaggelos, and A.V. Sahakian, "Linear-quadratic noise-smoothing filters for quantum-limited images", *IEEE Trans. Image Processing*, **4**, pp. 1328-33, 1995.
5. J.A. Fessler, "Penalized weighted least-squares image reconstruction for positron emission tomography", *IEEE Trans. Med. Imaging*, **13**, pp. 290-300, 1994.
6. J.A. Fessler, "Tomographic reconstruction using information-weighted spline smoothing", in *Information. Proc. in Med. Imaging*, H.H. Barrett and A.F.Gmitro, Eds. Heidelberg: Springer-Verlag, pp. 372-386, 1993.
7. J.A. Fessler and W.L. Rogers, "Spatial resolution properties of penalized-likelihood image reconstruction: space-invariant tomographs", *IEEE Trans. Image Processing*, **5**, pp. 1346-1358, 1996.
8. J.A. Fessler. "Nonparametric fixed-interval smoothing with vector splines", *IEEE Trans. Sig. Proc.*, **39**, pp. 852-859, 1991
9. B.R. Hunt and O. Kübler, "Karhunen-Loeve multi-spectral image restoration, part I: theory", *IEEE Trans. Acoustics, Speech, and Signal Processing*, **ASSP-32**, pp. 592-600, 1984.
10. J.B. Lee, A.S. Woodyatt, and M. Berman, "Enhancement of high spectral resolution remote-sensing data by a noise-adjusted principal components transform", *IEEE Trans. Geosci. Remote Sensing*, **28**, pp. 295-304, 1990.
11. M.N. Wernick, E.J. Infusino, and C.M. Kao, "Fast optimal pre-reconstruction filters for dynamic PET", *Conference Record of the IEEE NSS and MIC*, 1997.
12. M.N. Wernick, E.J. Infusino, and M. Milosevic, "Fast Spatio-temporal image reconstruction for dynamic PET", *IEEE Trans. Med. Imaging*, **18**, pp. 185-195, 1999.
13. M. Péligrini, H. Benali, G. El Fakhri, and *et al*, "Two-dimensional statistical model for regularized backprojection in SPECT", *Phys. Med. Biology*, **43**, pp. 421-434, 1998.
14. H. Lu, Z. Liang, D. Chen, and *et al*, "A combined transformation of ordering SPECT sinograms for signal extraction from measurements with Poisson noise", *SPIE Proc.*, **4322**, pp. 1431-1438, 2001.
15. P.J. La Rivière and X. Pan, "Nonparametric regression sinogram smoothing using a roughness-penalized Poisson likelihood objective function", *IEEE Trans. Med. Imaging*, **19**, pp. 773-786, 2000.
16. D.F. Yu nd J.A. Fessler, "Three-dimensional non-local edge-preserving regularization for PET transmission reconstruction", *Conference Record of the IEEE NSS and MIC*, 2000.